

Modeling and analysis of a bimorph piezoelectric cantilever beam for voltage generation

To cite this article: J Ajitsaria *et al* 2007 *Smart Mater. Struct.* **16** 447

View the [article online](#) for updates and enhancements.

Related content

- [A review of power harvesting using piezoelectric materials \(2003–2006\)](#)
Steven R Anton and Henry A Sodano
- [An experimental comparison between several active composite actuators for powergeneration](#)
Henry A Sodano, Justin Lloyd and Daniel J Inman
- [Modeling and characterization of MEMS-based PHDs](#)
T M Kamel, R Elfrink, M Renaud et al.

Recent citations

- [A new nonlinearly tapered FGM piezoelectric energy harvester](#)
Alireza Keshmiri *et al*
- [A groove engineered ultralow frequency piezomems energy harvester with ultrahigh output voltage](#)
Zoheir Kordrostami and Sajjad Roohizadegan
- [Henry A. Sodano *et al*](#)

Modeling and analysis of a bimorph piezoelectric cantilever beam for voltage generation

J Ajitsaria¹, S Y Choe¹, D Shen² and D J Kim²

¹ Department of Mechanical Engineering, Auburn University, Auburn, AL 36849, USA

² Materials Research and Education Center, Auburn University, Auburn, AL 36849, USA

E-mail: ajitsjk@auburn.edu and choeson@auburn.edu

Received 3 July 2006, in final form 12 December 2006

Published 14 February 2007

Online at stacks.iop.org/SMS/16/447

Abstract

Piezoelectric materials (PZT) have shown the ability to convert mechanical forces into an electric field in response to the application of mechanical stresses or vice versa. This property of the materials has found extensive applications in a vast array of areas including sensors and actuators. The study presented in this paper targets the modeling of a PZT bender for voltage and power generation by transforming ambient vibrations into electrical energy. This device can potentially replace the battery that supplies the power in a microwatt range necessary for operating sensors and data transmission. One of the advantages is that it is maintenance-free over a long time span.

The feasibility of this application has been repeatedly demonstrated in the literature, but a real demonstration of a working device is partially successful because of the various design parameters necessary for a construction of the PZT bender. According to a literature survey, the device can be modeled using various approaches. This paper focuses on the analytical approach based on Euler–Bernoulli beam theory and Timoshenko beam equations for the voltage and power generation, which is then compared with two previously described models in the literature: the electrical equivalent circuit and energy method. The three models are then implemented in a Matlab/Simulink/Simpower environment and simulated with an AC/DC power conversion circuit. The results of the simulation and the experiment have been compared and discussed.

(Some figures in this article are in colour only in the electronic version)

1. Introduction

Piezoelectric materials have found widespread application as transducers that are able to change electrical energy into mechanical motion or force or vice versa. The ability of piezoelectric materials to convert mechanical energy into electrical energy can provide a medium to transfer ambient motion (usually vibration) into electrical energy that may be stored and utilized by electronic devices such as sensors and wireless transmitters. Analytical modeling is an inevitable element in the design process to understand various interrelated parameters and to optimize the key design parameters while studying and implementing such power harvesting devices.

Previous publications and patents indicate the extensive application potential of a PZT (lead zirconate titanate) power harvesting device as a prospective replacement for the batteries currently employed. The electrical and mechanical behavior of the PZT power harvesting device has been studied by employing various approaches.

Umeda *et al* [1] were among the pioneers to study the PZT generator and proposed an electrical equivalent model being converted from mechanical lumped models of a mass, a spring and a damper that describe a transformation of the mechanical impact energy into electrical energy in the PZT material. Ramsay and Clark [2] considered the effects of transverse force on the PZT generator in addition to the force

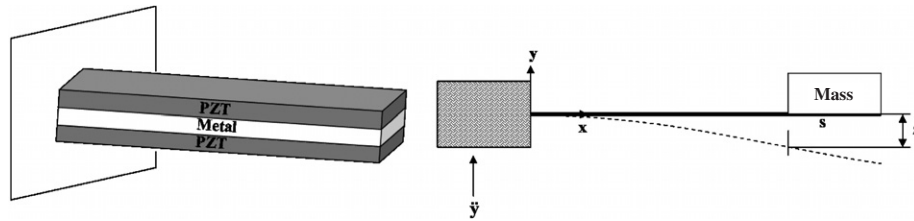


Figure 1. A schematic diagram of a PZT cantilever beam.

applied in the poling direction. Kasyap *et al* [3] formulated a lumped element model that represents the dynamic behavior of the PZT device in multiple energy domains and replace them with electric circuit components. The model has been experimentally verified by using a one-dimensional beam structure. Gonzalez *et al* [4] analysed the prospect of the PZT based energy conversion, and suggested several issues to raise the electrical output power of the existing prototypes to the level being theoretically obtained.

Smits and Chio [5] studied the electromechanical characteristics of a heterogeneous piezoelectric bender subject to various electrical and mechanical boundary conditions based on internal energy conservation. However, the model used does not provide any formulation for the voltage generation. Other authors such as Huang *et al* [6] and DeVoe *et al* [7] did the displacement and tip-deflection analysis along the beam and made a comparison with the experimental results. However, both proposals were limited to the actuator mode.

Hwang and Park [8] introduced a new model that is extracted from the calculation of the FEM (finite element method) and calculated the static responses of a piezoelectric bimorph beam in a piezoelectric plate element. However, no comparison has been made with experiments. Williams *et al* [9] analysed a PZT structure by using a single degree of freedom mechanical model. However, the model did not extend to a bimorph multilayer structure. Roundy *et al* [10–12] presented a slightly different approach based on the electrical equivalent circuit to describe the PZT bender, which leads to fair matches with the experimental results. However, the analysis only considered a low- g ($1\text{--}10\text{ m s}^{-2}$) vibration condition and lacks mechanical dynamics of the structure. Other authors (Lu *et al* [13]) improved the electrical model by adding an electro-mechanical coupling that represents a dynamic behavior of the beam vibrating under a single degree of freedom. Eggborn [14] developed the analytical models to predict the power harvesting from a cantilever beam and a plate using Bernoulli-beam theory and made a comparison with the experimental result. However, the structure used in the study does not have a proof mass attached at the end of the beam. Kim [15] analysed the unimorph and bimorph diaphragm structure for power generation using energy generation and piezoelectric constitutive equations. However, this study was limited to only diaphragm structures that were optimized through numerical analysis and FEM simulation at higher acceleration conditions. Shen *et al* [16] investigated the parameters influencing the output energy of a piezoelectric bimorph cantilever beam with a proof mass, where the resonant frequency and robustness of a cantilever structure

are considered for enhancing power conversion efficiency and implementing devices at high acceleration conditions.

The above studies have all had some success in modeling the PZT cantilever beam for voltage and power generation. However, many issues such as extensive theoretical analysis of a bimorph piezoelectric power generator based on a cantilever beam structure with proof mass attached at the end have not been addressed fully and lacks the modeling of power conversion circuitry. In this paper, special emphasis has been given to the analytical modeling of a bimorph PZT bender with a proof mass in the generator mode. The mathematical models developed are implemented in Matlab/Simulink with AC/DC power conversion circuitry. Models developed for this application are then compared with the experimental results to assess the accuracy of the various models.

2. Mathematical models

Several different modeling approaches have been applied to study the dynamic characteristics of the structure. Most of the works published have applied an electric equivalent circuit to represent the mechanical characteristics of the structure, which does not fully reflect the actual dynamics of the structure. Euler–Bernoulli beam theory has also been previously studied for a unimorph structure but has been limited to modeling in the actuation mode. Thus, a new approach based on a combination of Euler–Bernoulli beam theory and Timoshenko beam equations has been developed for the bimorph PZT bender taking into account material properties and coupled with the power conversion circuit. Figure 1 shows a schematic diagram of a PZT cantilever beam.

The following section describes the development of the three mathematical models previously mentioned for the device. The first model is based on an electrical equivalent circuit for a mechanical lumped model. The second one combines the Euler–Bernoulli beam theory and Timoshenko beam equations. The final one uses the conservation of energy in the beam in conjunction with a mechanical single degree of freedom model.

2.1. Electrical equivalent circuit

The study of the transient dynamic characteristics of a PZT bender utilizing electrical equivalent models has been performed in previous studies and the model has shown fair accuracy in various conditions of mechanical stress [10–13]. The electrical equivalent model has been studied and implemented in this research effort to compare the accuracy

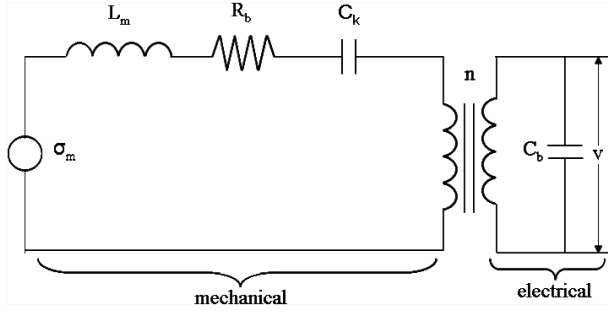


Figure 2. Circuit representation of a PZT beam [11].

and validity of the experimental results and the analytical results from the models based on beam theory and energy conservation. Figure 2 shows an electric equivalent circuit model for a PZT beam [11], where a voltage source is connected in series with an inductor, a resistor and a capacitor that build a resonant circuit. The transformer represents the voltage adaptation while the capacitor indicates the inherent capacitance of the device.

The circuit can be described by using Kirchhoff's voltage law:

$$\sigma_{in} = L_m \ddot{\varepsilon} + R_b \dot{\varepsilon} + \frac{\ddot{\varepsilon}}{C_k} + nV \quad (1)$$

$$i = C_k \dot{V}. \quad (2)$$

The equivalent circuits leads to the correlation between the strain ε and voltage V [12];

$$\ddot{\varepsilon} = \frac{-Y}{k_1 k_2 m} \varepsilon - \frac{b_m}{k_1 m} \dot{\varepsilon} + \frac{Y}{k_1 k_2 m} \frac{d_{31}}{2t_c} V + \frac{\ddot{y}}{k_2}, \quad (3)$$

and

$$V = \frac{n_p t_c d_{31} Y}{\varepsilon} \dot{\varepsilon} \quad (4)$$

where

$\ddot{\varepsilon}, \dot{\varepsilon} \rightarrow$ second and first time derivative of strain.

2.2. Beam theory (Timoshenko and Euler–Bernoulli)

The static analysis of a piezoelectric cantilever sensor is typically performed by the use of calculations employed for deflection of a thermal bimorph proposed by Timoshenko [5–7]. The principle is based on the strain compatibility between three cantilever beams joined along the bending axis. Due to forces applied by one or all of the layers, the deflection of the three-layer structure is derived from a static equilibrium state. The structure considered is a piezoelectric heterogeneous bimorph, where two piezoelectric layers are bonded on both sides of a purely elastic layer, i.e. brass.

Figure 3 shows a basic geometry of the three-layer multimorph. Brass with a pure elasticity is sandwiched between the upper and lower layers of the PZT material. The modeling of this structure neglects shear effects and ignores residual stress-induced curvature. In addition, the beam thickness is much less than the piezoelectric-induced curvature, so the second-order effects such as electrostriction can be ignored.

Moreover, the radius of curvature for all the layers is assumed to be approximately the same to those of the structure, simply because of the assumption that the thickness is much less than the overall beam curvature.

The total strain at the surface of each layer is the sum of the strains caused by the piezoelectric effect, the axial force, and the bending. It is noted that the sign of the surface strain depends on the bending of either the top or bottom surface of the layer:

$$\varepsilon_i = \varepsilon_{piezo} + \varepsilon_{axial} + \varepsilon_{bend} = d_{31} E_i + \frac{F_i}{A_i Y_i} \pm \frac{t_i}{2r} \quad (5)$$

where ε_{piezo} in the linear constitutive equation above considers the transverse piezoelectric coupling coefficient d_{31} and the electric field across the thickness of the layer E_i . for a piezoelectric material, t_1 and t_3 are the thickness of the PZT layer and t_2 is the thickness of the center shim, A_i is the area of the corresponding layer and Y_i is the Young's modulus of elasticity.

Hence the radius of curvature is given by the term

$$\frac{1}{r} = \frac{2d_{31} D A^{-1} C}{2 - D A^{-1} B} \quad (6)$$

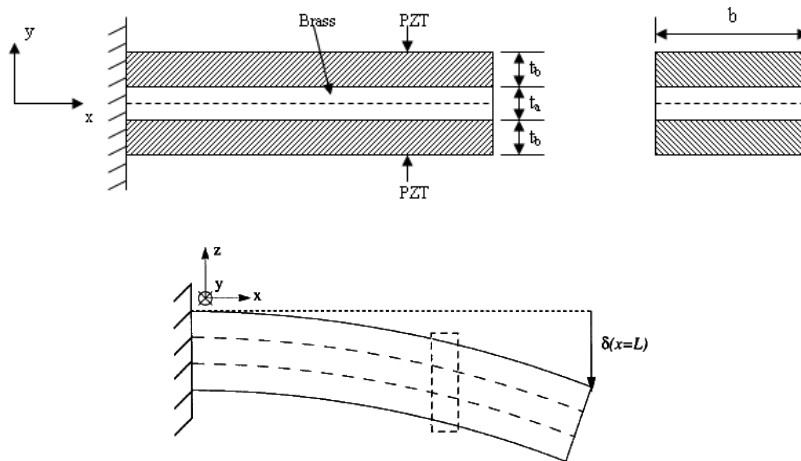


Figure 3. Geometry of the beam [7].

where

$$A = \begin{bmatrix} \frac{1}{A_1 Y_1} & -\frac{1}{A_2 Y_2} & 0 \\ 0 & \frac{1}{A_2 Y_2} & -\frac{1}{A_3 Y_3} \\ 1 & 1 & 1 \end{bmatrix}, \quad B = \begin{bmatrix} t_1 + t_2 \\ t_2 + t_3 \\ 0 \end{bmatrix},$$

$$C = \begin{bmatrix} -E \\ E \\ 0 \end{bmatrix}.$$

On the other hand, Euler–Bernoulli beam theory describes the relationship between the radius of curvature and the force applied, which is given by the following equation [14]

$$\rho A \frac{\partial^4 w(x, t)}{\partial t^4} + YI \frac{\partial^4 w(x, t)}{\partial x^4} = F(t) \quad (7)$$

where ρ is the density, I is the moment of inertia and $F(t)$ is the applied force.

A general solution for this equation is given by

$$w(x, t) = \sum q_i(t) X_i(x) \quad (8)$$

where the displacement and the vibration is expressed in the case of a cantilever beam as follows:

$$X_i(x) = \cosh(\beta_i x) - \cos(\beta_i x) - \frac{\sinh(\beta_i L) - \sin(\beta_i L)}{\cosh(\beta_i L) + \cos(\beta_i L)} \times (\sinh(\beta_i x) - \sin(\beta_i x)) \quad (9)$$

$$q_i(t) = \frac{1}{\omega_{di}} e^{-\zeta \omega_{ni} t} \int_0^t F_i(\tau) e^{-\zeta \omega_{ni} \tau} \sin(\omega_{di}(t - \tau)) d\tau \quad (10)$$

and

$$\beta_i^4 = \frac{\omega_{ni}^2}{C^2} \quad (11)$$

ω_n , is the natural frequency obtained by solving the transcendental equation:

$$\cosh(\beta_i L) \cos(\beta_i L) + 1 = 0. \quad (12)$$

The radius of curvature is given by the following equations:

$$r = \frac{1}{2w(L)} L^2, \quad \text{where } \frac{1}{r} = \dot{w}(x) \text{ and } w(x) = \frac{1}{2r} x^2.$$

Hence by substituting the radius of curvature term in equation (6), the voltage produced for the PZT bender is given by:

$$V = \frac{2w(L)t_p}{L^2} \frac{2 - DA^{-1}B}{2d_{31}DA^{-1}} \begin{bmatrix} -1 \\ 1 \\ 0 \end{bmatrix}^{-1}. \quad (13)$$

2.3. Conservation of energy

The principle is based on the fact that the total energy of the PZT bender stored is equal to the sum of the mechanical energy applied to the beam and the electrical energy on the charges being applied by the electric field [15, 17, 18]. When a mechanical stress is applied, the energy stored in a PZT layer is the sum of the mechanical energy and the electric-field-induced energy. Thus, the energy stored in a PZT layer is expressed as follows:

$$U_u = \frac{1}{2}(s_{11}^E \sigma_1 - d_{31} E_3) \sigma_1 = \frac{1}{2} s_{11}^E \sigma_1^2 \quad (14)$$

where σ is the stress and s is the stiffness matrix.

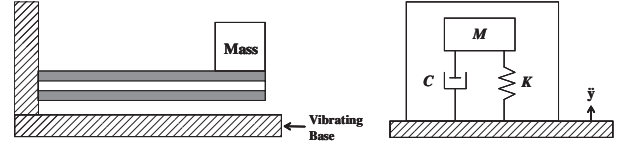


Figure 4. Sensor structure and equivalent SDOF model.

On the other hand, the energy in the metal layer can be expressed by a simple equation because of the lack of the electric field as follows:

$$U_m = \frac{1}{2} s_m \sigma_1^2. \quad (15)$$

The total energy of the beam is given as [15]:

$$U_{\text{total}} = \int_0^L \int_0^W \left(\int_{\frac{t_2}{2}}^{\frac{t_2}{2}+t_1} dU_u dz + \int_{-\frac{t_2}{2}}^{\frac{t_2}{2}} dU_m dz + \int_{-\frac{t_2}{2}-t_3}^{-\frac{t_2}{2}} dU_l dz \right) dy dx. \quad (16)$$

On the other hand, the electric field is given by $E = V/(2t_3)$.

The total electrical energy is equal to a product of the charge and the voltage. Thus, the charge generated in the beam is obtained by a partial derivative of the total energy with respect to the voltage:

$$Q = \frac{\partial U_{\text{total}}}{\partial V} = -3 \frac{d_{31} s_m (t_2 + t_3) L^2}{X} F_o. \quad (17)$$

The capacitance of the piezoelectric material is described as the relation between the voltage and charge on the piezoelectric material. Hence the capacitance C_{free} of the beam can be found, where no load is applied [15]:

$$C_{\text{free}} = \frac{v_{33}^T W L}{2t_3} \left(1 + \frac{(6s_m t_3 (t_2 + t_3)^2 - X)}{X} K_{31}^2 \right) \quad (18)$$

where K_{31} is the coupling coefficient

Thus, the voltage generated is found as a function of the applied force:

$$V = \frac{Q}{C_{\text{free}}} = - \frac{6d_{31} s_m t_3 (t_2 + t_2) L}{v_{33}^T W X (1 + (\frac{6s_m t_3 (t_2 + t_3)^2}{X} - 1) K_{31}^2)} F_o. \quad (19)$$

The schematic structure of a sensor is shown in figure 4, where a mass (M_{end}) is attached to the free end of the bimorph PZT cantilever beam that is fixed to a vibrating base. Both the piezoelectric bending composite beam and M_{end} are assumed to be rigid bodies with no elastic coupling. Then, the structure can be modeled with a single degree of freedom (SDOF) system, which solely consists of a proof mass M , a spring with stiffness K , a damper with damping coefficient C and a vibrating base. The resulting equivalent model is shown in figure 4. Hence, $y(t)$ is the motion of the vibrating base, and $z(t)$ is the relative motion between the vibrating base and the proof mass M , assumed to be a point mass with equivalent vertical force at the free end of the sensor. Thus, the mass can be expressed by the following equation [19]:

$$M = \frac{33}{140} M_{\text{beam}} + M_{\text{end}} \quad (20)$$

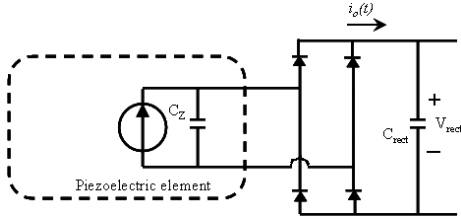


Figure 5. A simplified circuit representation.

where M_{beam} is the mass of the beam and M_{end} is the end mass.

According to Newton's second law, the mechanical model is derived as follows:

$$M\ddot{z} + C\dot{z} + Kz = -M\ddot{y}. \quad (21)$$

A transfer function between the input acceleration and the output displacement can be obtained in the Laplace plane with initial conditions $z(0) = \dot{z} = 0$, where $\omega_n = \sqrt{\frac{K}{M}}$, $\zeta = \text{damping_ratio}$:

$$\left| \frac{Z(s)}{\ddot{Y}(s)} \right| = \frac{1}{s^2 + (2\zeta\omega_n)s + \omega_n^2}. \quad (22)$$

So, the response of the force F_o at the beam is obtained after $Z(t)$ and $\ddot{Z}(t)$ are solved from the equation to get

$$F_o(t) = M_{\text{end}} \times \ddot{Z}(t). \quad (23)$$

All of the models described above are solved by using Matlab/Simulink. Simulation results are compared with the experimental results in the following sections:

$$V = -\frac{6d_{31}s_mt_3(t_2+t_3)L}{v_{33}^T W X (1 + (\frac{6s_mt_3(t_2+t_3)^2}{X} - 1)K_{31}^2)} M_{\text{end}} \times \ddot{Z}(t). \quad (24)$$

3. Electrical circuit

The analytical models and the analysis based on a simple resistive load are not a very realistic approximation of the actual electrical load. In reality, the electrical system would look something like the circuit shown in figure 5. The equivalent mechanical side of the circuit is exactly the same as shown in figure 2. The development of a model for this case is useful in that it represents a more realistic operating condition.

The major components involved in this circuit are AC/DC rectifier and a filter capacitor. The AC/DC rectifier converts the AC signal from the piezo-source into DC current and the filter capacitor smooths the electrical flow.

4. Experiments

The bender was composed of a brass center shim sandwiched by two layers made of a sheet of PZT-5A. The thickness of the brass plate and the PZT are 0.134 and 0.132 mm, respectively, and the attached mass is made from tungsten.

In order to investigate parameters of the prototype structure, a test stand is built to excite the bender with a predetermined resonant frequency. The system described here is designed to utilize the z -axis vibration as the only vibration source for the device. The cantilever is excited by a shaker connected to a function generator via an amplifier. For a characterization of the fabricated cantilever device, the voltage generated was evaluated by connecting a resistor. Figure 6 illustrates the schematic of the experimental set-up and a photo for a real set-up.

5. Results and discussion

The accuracy of the model was compared against experimental results to demonstrate the ability of the model to accurately predict the amount of power produced by the PZT generator when subjected to transverse vibration. To ensure that the model and experimental tests were subjected to the same excitation force an accelerometer was used to calculate the amplitude of the sinusoidal force applied to the beam. The beam was excited by a sinusoidal input and the steady state power output was measured across several different resistors. In order to examine the models, the power generated by the piezoelectric prototypes were compared and evaluated. Three cases have been studied with an open circuit, a resistive load without and with a rectifier with a capacitor.

5.1. Open circuit

The output voltage waveforms obtained from the simulation and the experiments performed on the PZT bender are compared in figure 7. The experimental results show 11.49 V, while the models give 10.47, 11.649 and 10.254 V. Secondly, the phase displacements vary in a range of more than 90°.

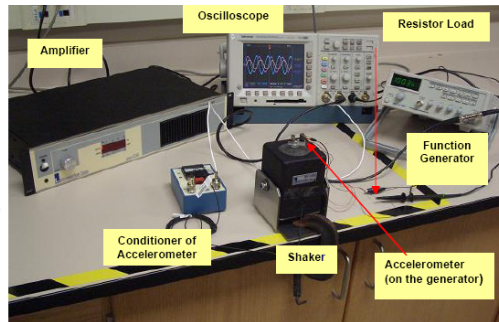
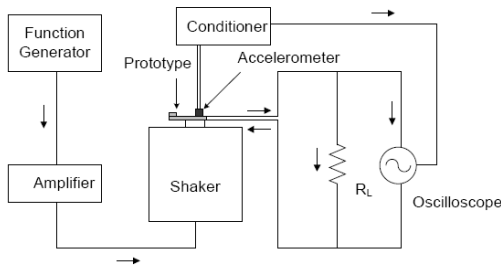


Figure 6. Schematic and photo of the experimental set-up with a resistance load.

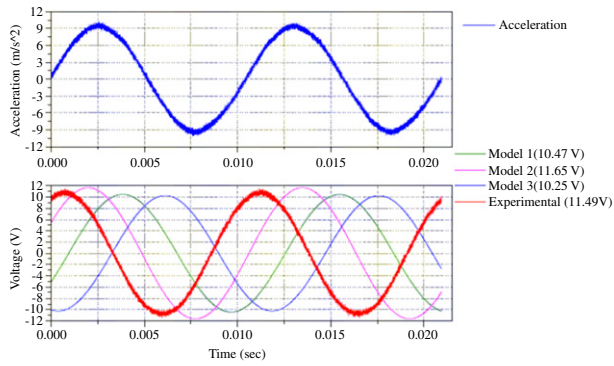


Figure 7. Comparison of the amplitude of the open circuit AC voltage for three models with experimental results.

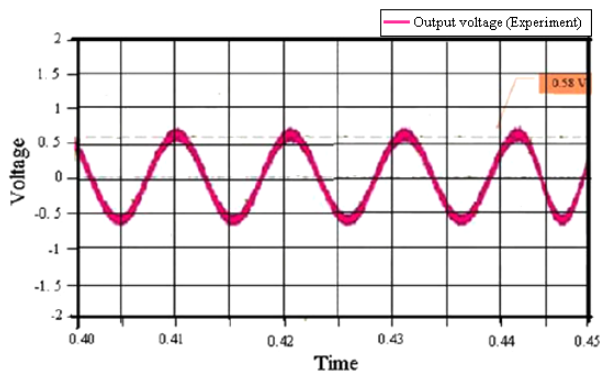


Figure 8. Experimental results for the output voltage with a 4 kΩ resistive load.

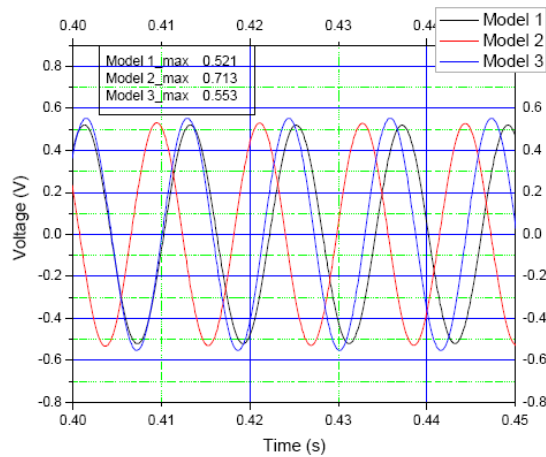


Figure 9. Simulation results for the output voltage with a 4 kΩ resistive load.

The predicted response shown in the figure shows a transient response for a small period of time while the experimental results do not because they were recorded at steady state vibration. The results indicate that the models provide a very accurate measurement of the open circuit voltage generated.

5.2. Resistive load

Figures 8 and 9 show the output waveform of the PZT power generator measured and simulated, where a 4 kΩ resistor is

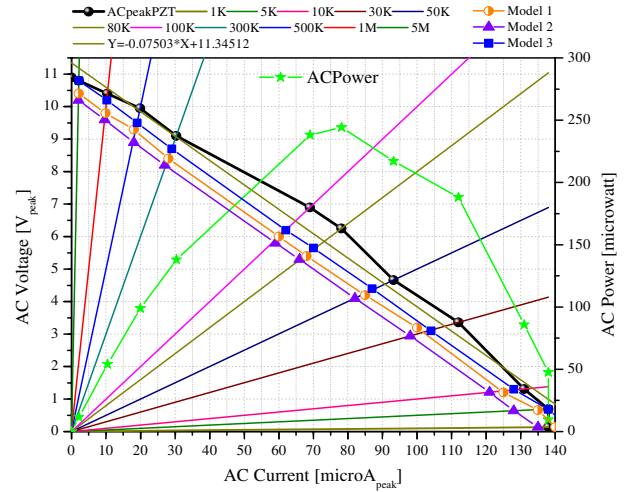


Figure 10. I - V characteristics of the PZT bender without rectifier circuit.

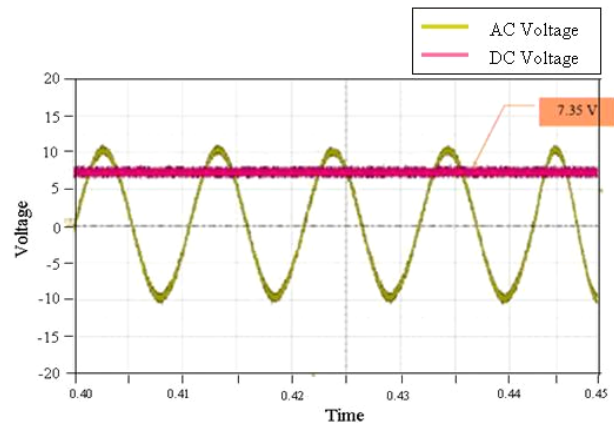


Figure 11. DC voltage at a 400 kΩ resistive load.

connected as a load. The peak voltage measured amounts to 0.58 V, while the simulated voltages are 0.521, 0.713 and 0.553 V for the three models, respectively.

When the value of the resistor increases, the current drawn from the PZT generator decreases, resulting in the increase in voltage. Figure 10 shows the I - V characteristic of the bender for different resistive loads. This I - V curve plays a significant role in selecting a topology for the circuit and, at the same time, sizing components. The charge generated at a constant acceleration decreases when the current increases. The maximum power of the device produced by the PZT bender is about 250 μ W approximately at a load resistance of 110 kΩ. The device is comparable to a voltage source with an internal resistance, which generates the maximum power when the value of the internal resistor is identical with the one of the load resistor.

The experiments undertaken demonstrate that the designed system can supply a maximum power of 250 μ W at 110 kΩ resistive load when the PZT bender is excited with a vibration with an amplitude of 9.8 m s⁻² (1g) at 97.6 Hz. The phase shift amounts to 52° between the input acceleration and the AC output voltage. In contrast, the voltage and input

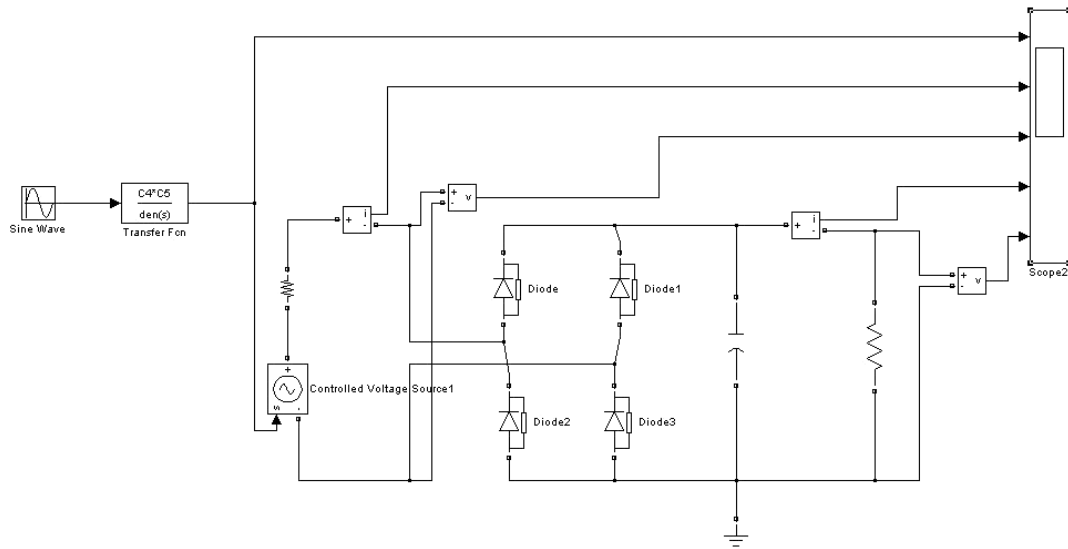


Figure 12. Simulation with Matlab/Simulink/Simpower.

acceleration for the first model is in phase, the second one 62° and the third one around 125° , respectively.

5.3. Resistive load with rectifier

Multi-run simulations have been carried out to compare both results. The model of the PZT beam is integrated into Simpower by using a controlled voltage source. Figure 11 shows the waveform of the voltages before and after the rectifier for a $400\text{ k}\Omega$ resistive load. The DC voltage amounts to 7.35 V and the AC voltage ripples are well suppressed.

Figure 12 shows an integrated model with a PZT bender, a bridge rectifier with a capacitor and a resistor that has been implemented in Matlab/Simulink/Simpower.

Figure 13 shows simulated results for AC voltage and AC current, and DC voltage for the transverse vibration of amplitude $1g$ at the resonance frequency of the PZT bender. It is noted that the AC voltage clamps whenever the current starts to flow. It can also be interpreted that a voltage drop at the internal resistance drastically increases as soon as a current flows. It is noted that the current charging the DC capacitor is not sinusoidal and the influence of the current has been worsened at a resistive load with a rectifier compared to the previous case.

6. Conclusion

One method of performing power harvesting is to use PZT materials that can convert the ambient vibration energy surrounding them into electrical energy. This electrical energy can then be used to power other devices or stored for later use. The need for power harvesting devices is caused by the use of batteries as power supplies for wireless electronics. As the battery has a finite lifespan, once depleted of its energy, the sensor must be recovered and the battery replaced for the continued operation of the sensor. This practice of obtaining sensors solely to replace the battery can become an expensive task. Therefore, methods of harvesting the energy around these

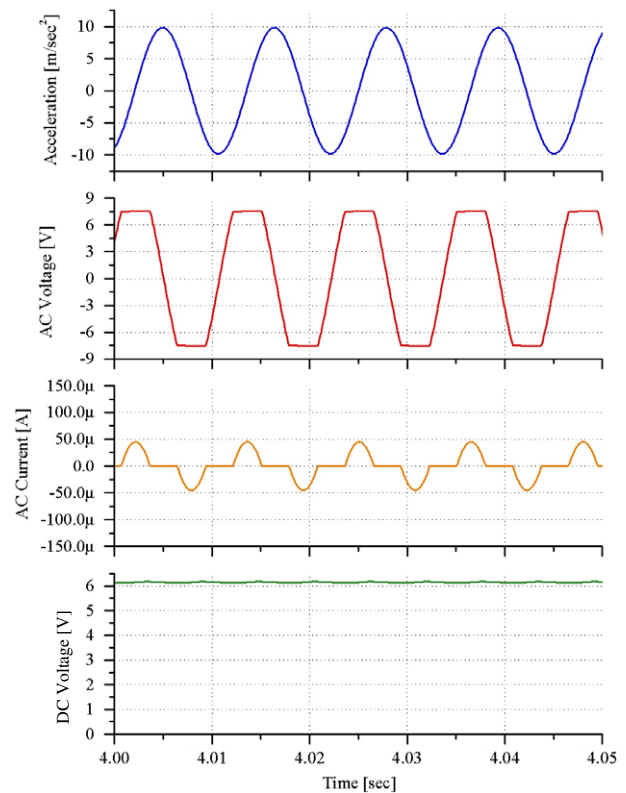


Figure 13. AC voltage and current, and DC voltage at a $400\text{ k}\Omega$ resistive load with a rectifier.

sensors must be implemented to expand the life of the battery or ideally provide an endless supply of energy to the sensor over its lifetime.

A PZT bender with a bimorph structure is designed for power generator. The 31 mode operation for the material is chosen because of the higher strain and lower resonant frequencies compared to those in the 33 mode operation. The work presented has been focused on modeling of the PZT

materials in a cantilever beam structure and analyses of the device in conjunction with a power conversion circuit.

We have developed a model to predict the amount of power capable of being generated through the vibration of a cantilever beam with attached PZT elements. The derivation of the model has been provided with boundary conditions. The model was verified using experimental results and proved to be very accurate independent of load resistance. In addition, the verification of the model was performed on a bimorph PZT bender, indicating that the model is robust and can be applied to a variety of different mechanical conditions. The model developed provides a design tool for developing power harvesting systems by assisting in determining the size and extent of vibration needed to produce the desired level of power generation. The potential benefits of power harvesting and the advances in low power electronics and wireless sensors are making the future of this technology look very bright.

References

- [1] Umeda M, Nakamura K and Ueha S 1996 Analysis of the transformation of mechanical impact energy to electric energy using piezoelectric vibrator *Japan. J. Appl. Phys.* **35** 3267–73
- [2] Ramsay M J and Clark W W 2001 Piezoelectric energy harvesting for bio-MEMS application *Smart Struct. Mater.* **4332** 429–38
- [3] Kasyap A *et al* 2002 Energy reclamation from a vibrating piezoceramic composite beam *9th Int. Congress on Sound and Vibration* vol 9
- [4] Gonzalez J L, Rubio A and Moll F 2001 Human powered piezoelectric batteries to supply power to wearable electronic devices *Int. J.-Soc. Mater. Eng. Resources* **10** 34–40
- [5] Smits J G and Choi W S 1991 The constituent equations of piezoelectric heterogeneous bimorphs *IEEE Trans. Ultrason. Ferroelectr. Freq. Control* **38** 256–70
- [6] Huang C, Lin Y Y and Tang T A 2004 Study on the tip-deflection of a piezoelectric bimorph cantilever in the static state *J. Micromech. Microeng.* **14** 530–4
- [7] DeVoe D L and Pisano A P 1997 Modeling and optimal design of piezoelectric cantilever microactuators *J. Microelectromech. Syst.* **6** 266–70
- [8] Hwang W S and Park H C 1993 Finite element modeling of piezoelectric sensors and actuators *AIAA J.* **31** 930–7
- [9] Williams C B and Yates RB 1996 Analysis of a micro-electric generator for microsystems *Sensors Actuators A* **52** 8–11
- [10] Roundy S and Wright P K 2004 A piezoelectric vibration based generator for wireless electronics *Smart Mater. Struct.* **13** 1131–42
- [11] Roundy S 2005 On the effectiveness of vibration-base energy harvesting *J. Intell. Mater. Syst. Struct.* **16** 809–23
- [12] Roundy S, Leland E S, Baker J, Carleton E, Reilly E, Lai E, Otis B, Rabaey J M, Wright P K and Sundararajan V 2005 Improving power output for vibration-based energy scavengers *IEEE Trans. Pervasive Comput.* **4** 28–36
- [13] Lu F, Lee H P and Lim S P 2004 Modeling and analysis of micro piezoelectric power generators for micro-electromechanical-systems applications *Smart Mater. Struct.* **13** 57–63
- [14] Eggborn T 2003 Analytical models to predict power harvesting with piezoelectric materials *Master's Thesis* Virginia Polytechnic Institute and State University
- [15] Kim S 2002 Low power energy harvesting with piezoelectric generators *PhD Thesis* University of Pittsburgh
- [16] Shen D, Ajitsaria J, Choe S Y and Kim D J 2006 The optimal design and analysis of piezoelectric cantilever beams for power generation devices *Mater. Res. Soc. Symp. Proc.* **888** V03-04.1–V03-04.6
- [17] Sodano H A, Park G and Inman D J 2004 Estimation of electric charge output for piezoelectric energy harvesting *Strain* **40** 49–58
- [18] Wang Q M and Cross L E 1999 Constitutive equations of symmetrical triple layer piezoelectric benders *IEEE Trans. Ultrason. Ferroelectr. Freq. Control* **46** 1343–51
- [19] Ng T H and Liao W H 2005 Sensitivity analysis and energy harvesting for a self-powered piezoelectric sensor *J. Intell. Mater. Syst. Struct.* **16** 785–97